The Astrophysical Journal, 670: L49–L51, 2007 November 20

DETECTION OF METHANE ON KUIPER BELT OBJECT (50000) QUAOAR

E. L. Schaller[1] and M. E. Brown[1]

Received 2007 September 6; accepted 2007 October 4; published 2007 October 25

ABSTRACT

The near-infrared spectrum of (50000) Quaoar obtained at the Keck Observatory shows distinct absorption features of crystalline water ice, solid methane, and ethane, and possibly other higher order hydrocarbons. Quaoar is only the fifth Kuiper Belt object (KBO) on which volatile ices have been detected. The small amount of methane on an otherwise water ice–dominated surface suggests that Quaoar is a transition object between the dominant volatile-poor small KBOs and the few volatile-rich large KBOs such as Pluto and Eris.

Subject headings: Kuiper Belt — planets and satellites: general

Online material: color figures

1. INTRODUCTION

While once Pluto and Triton were the only objects in the outer solar system known to contain volatile ices on their surfaces, the recent discoveries of frozen methane on the large Kuiper Belt objects (KBOs) Eris, Sedna, and 2005 FY9 have shown that these objects are part of a new class of surface volatile-rich bodies in the outer solar system (Brown et al. 2005; Licandro et al. 2006; Barucci et al. 2005; Brown et al. 2007). In contrast to these bodies with detectable volatiles, spectral observations of small KBOs over the past decade have found that most of these objects either contain varying amounts of involatile water ice on their surfaces or have flat spectra with no identifiable features (Barkume et al. 2008). To understand the dichotomy between volatile-rich and volatile-free surfaces in the outer solar system, Schaller & Brown (2007) constructed a simple model of atmospheric escape of volatile ices over the age of the solar system. They found that while most KBOs are too small and hot to retain their initial volatile ices to the present day, a small number are large and cold enough to retain these ices on their surfaces.

As anticipated, the model suggests that the largest KBOs, Eris, Pluto, and Sedna are all expected to retain surface volatiles, while the vast majority of the other known objects in the Kuiper Belt are expected to have lost all surface volatiles. Two known intermediate-sized KBOs are predicted to be in the transition region where they may have differentially lost some volatile ices (N_2) but retained others (CH_4). One of these transition objects, 2005 FY9, with a diameter of ~1450 km (Stansberry et al. 2007) does indeed appear to contain abundant CH_4 but be depleted in N_2.

The other object that appears to be in the volatile-nonvolatile transition region is Quaoar, with a diameter of 1260 ± 190 km (Brown & Trujillo 2004). The infrared spectrum of Quaoar does not resemble that of 2005 FY9, however. Quaoar's spectrum is dominated by absorptions due to involatile water ice, which is not detected at all on 2005 FY9. In addition, Jewitt & Luu (2004) reported the detection of an absorption feature near 2.2 μm that they attributed to ammonia hydrate. They also detected the presence of crystalline water ice, which, at the ~40 K radiative equilibrium temperature of Quaoar, is thought to be converted to amorphous water ice on a relatively short (~10 Myr) timescale by cosmic-ray bombardment. The crystallinity of the water ice and the detection of the 2.2 μm feature that they attributed to ammonia hydrate led Jewitt & Luu (2004) to suggest that Quaoar may have experienced relatively recent cryovolcanic activity.

In this Letter, we present a new infrared spectrum of Quaoar with a signal-to-noise ratio (S/N) in the K band 6 times greater than that of Jewitt & Luu (2004) and model the ices present on the surface.

2. OBSERVATIONS

Near-infrared spectra of Quaoar were obtained on 2002 July 12, and 2007 April 23, 24, and 25 using NIRSPEC, the facility medium- to high-resolution spectrometer on the Keck telescope (McLean et al. 1998). Three separate grating settings were used to completely cover the region from 1.4 to 2.4 μm. The 1.44–1.73 and 1.70–2.13 μm regions were each covered in six exposures of 200 s each, and the 2.0–2.4 μm region was covered in 82 exposures of 300 s each. Observations consisted of a series of exposures on two or three nod positions along the 0.57″ slit. All observations were performed at an air mass of better than 1.5. Data reduction was carried out as described in Brown (2000). Telluric calibration was achieved by dividing the spectra by nearby G dwarf stars observed at an air mass within 0.1 of that of the target.

Figure 1 shows the complete near-infrared spectrum of Quaoar. The absolute value of the infrared albedo is obtained from the R albedo of $0.092^{+0.036}_{-0.023}$ (Brown & Trujillo 2004), the $V - R$ color of 0.64 ± 0.04, and an estimated $V - J$ color of 2.1 ± 0.2 using typical values found by McBride et al. (2003). Errors in the overall absolute albedo calibration are of the order of 30% and are dominated by the uncertainty in the optical albedo.

The characteristic broad absorptions due to water ice are apparent at 1.5 and 2.0 μm. In addition, the presence of the unique crystalline water ice feature at 1.65 μm indicates that at least some of the water ice is in crystalline form. We also detect the absorption feature at 2.2 μm previously attributed to ammonia hydrate as well as a series of broad absorption features beyond 2.25 μm.

3. SPECTRAL MODELING

We first attempt to model the spectrum of Quaoar with a mixture of water ice and a dark featureless material. Using the bidirectional reflectance models of Hapke (1993), we model a spatially segregated mixture of crystalline water ice grains (Grundy & Schmitt 1998) and a dark red material. Optical path length was parameterized as a grain size in a scattering regolith.

[1] Division of Geological and Planetary Sciences, California Institute of Technology, Pasadena, CA 91125.

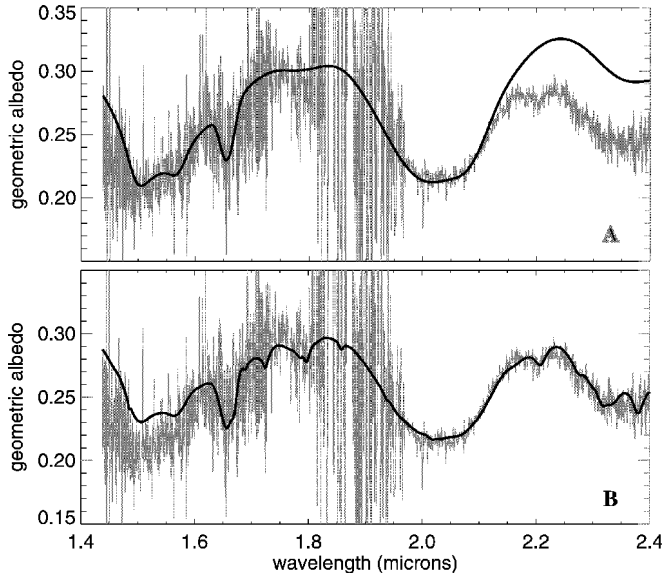

FIG. 1.—(*a*) Near-infrared spectrum of Quaoar obtained with NIRSPEC (McLean et al. 1998) on the Keck telescope. The signature of crystalline water ice is dominant. A best-fit water ice and dark red continuum model is shown. The major features of the spectrum are well fit by the model except for the 2.2–2.4 μm region, where additional absorption occurs. (*b*) Quaoar spectrum shown with the best-fit water ice, continuum, methane, and ethane model. The presence of methane is required to fit the long wavelength end of the spectrum. [*See the electronic edition of the Journal for a color version of this figure.*]

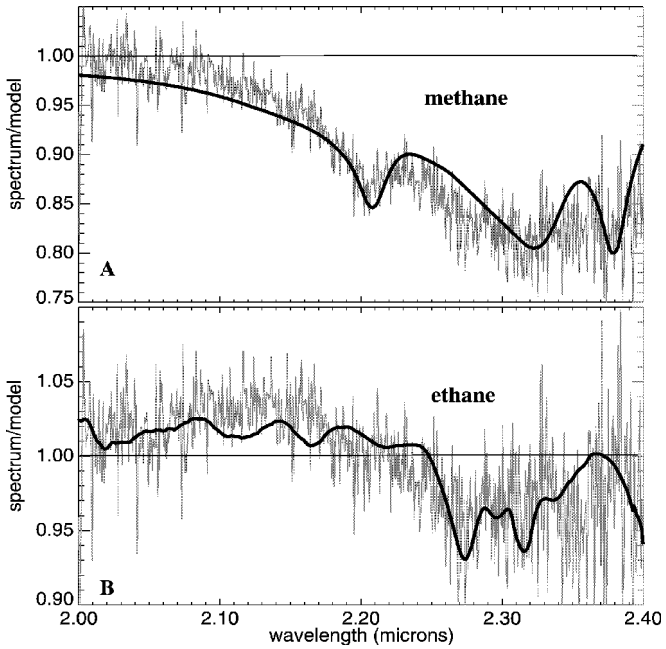

FIG. 2.—(*a*) Ratio of the spectrum to the best-fit water ice and red continuum model. In addition to the 2.2 μm feature seen by Jewitt & Luu (2004), we see additional distict but broader absorption features at 2.32 and 2.38 μm that are well matched by methane. A model methane spectrum (Grundy et al. 2002) with 100 μm grain sizes provides an excellent fit to the ratio spectrum. (*b*) Ratio of the spectrum to the best-fit water ice, continuum, and methane model. While most features of the spectrum are well fit by this model, additional absorptions occur near 2.3 μm. The two strongest absorption features at 2.27 and 2.32 μm are well fit by ethane. [*See the electronic edition of the Journal for a color version of this figure.*]

In order to investigate the additional absorption features longward of 2.1 μm not due to water ice, we performed a least-squares best fit to the 1.4–2.1 μm region where the fractional abundance of the ice, the grain size of the ice, and the color of the dark material were allowed to vary. Figure 1*a* shows the best-fit model with 10 μm water ice grain sizes, an ice fraction of 40% linearly mixed with a red continuum with a spectral slope of 10% per μm, and an albedo of 13% at 2 μm. The spectrum could be equally well fit with a model where water ice was significantly more abundant and the dark material was intimately mixed, rather than linearly mixed, with the ice.

The water ice model provides a good fit to the data from 1.4 to 2.1 μm and, as expected, deviates in the region beyond 2.1 μm. In order to explore the spectral shape of the deviation beyond 2.1 μm, we show, in Figure 2*a*, the ratio of the Quaoar spectrum to the water ice model. In addition to the 2.2 μm feature seen by Jewitt & Luu (2004) we see additional distinct but broader absorption features at 2.32 and 2.38 μm. The locations and depths of these three absorption features as well as the general shape of the ratio spectrum beyond 2.1 μm are well fit by absorptions due to methane ice. A model methane spectrum using the laboratory data of Grundy et al. (2002) with 100 μm grain sizes provides an excellent fit to the 2.0–2.4 μm ratio spectrum. In addition, smaller absorptions at 1.8 and 1.72 μm are also well fit by methane (Fig. 1*b*). We measured the band center of the 2.2 μm feature to be at 2.205 $\pm$ 0.002, which is consistent with that expected from pure methane (Quirico & Schmitt 1997). Hydrated ammonia, in contrast, has a single absorption in this region at a wavelength between 2.21 and 2.24 μm, depending on the degree of hydration (Moore et al. 2007). While the Quaoar absorption feature at 2.205 $\pm$ 0.002 is perhaps consistent with the 2.21 μm wavelength of the absorption feature of the most hydrated ammonia, ammonia cannot explain any of the additional major absorptions seen on Quaoar, all of which are well explained by the presence of methane. We thus conclude that the absorption feature initially attributed to ammonia is actually one of a series of absorption features caused by methane.

We can model the overall spectrum of Quaoar with a linear mixture of 35% water ice, 5% methane, and 60% dark material. While most features of the spectrum are well fit by this model, additional absorptions near 2.27 μm still cannot be explained by methane (Fig. 2*b*). On 2005 FY9, Brown et al. (2007) found that the surface contained not just volatile methane, but a small amount of involatile ethane, hypothesized to derive from irradiation of the solid methane. The deviation from the methane spectrum on Quaoar also appears to be well fit, at least in part, by the presence of ethane. Figure 2*b* shows a model of 10 μm ethane grains constructed from the absorption coefficients of Quirico & Schmitt (1997). In particular, the two strongest absorption features at 2.27 and 2.32 μm are clearly detected as they are on 2005 FY9. An additional small absorption feature at 2.36 μm remains unidentified but may be due to a higher order hydrocarbon.

Figure 1*b* shows the complete model fit with a spatial mixture of 35% water ice, 55% dark material, 6% methane, and 4% ethane. While the specific values of these parameters have little unique meaning, as many different values could give similar fits, in general we find that methane and ethane are minority species on a water ice dominated surface. The slight increase in the albedo of our best-fit model in the 1.4–1.6 μm region compared to the spectrum indicates that a single sloped continuum in the infrared is insufficient. No evidence for other volatile species is detected; in particular, we did not detect the 2.148 μm N2 absorption feature nor the 2.352 μm CO absorption feature.

4. DISCUSSION

With significantly higher S/N in the 2.0–2.4 μm region, the 2.2 μm absorption feature on Quaoar previously identified as ammonia hydrate (Jewitt & Luu 2004) is clearly seen to be due to methane ice. No compelling evidence is seen for the presence of ammonia. The presence of crystalline water ice on the surface of Quaoar still remains unexplained because it is expected that ice should currently exist in the amorphous form on the ~40 K surface of Quaoar. However, the presence of the 1.65 μm absorption feature due to crystalline water ice in the spectrum of every well-observed water ice–rich KBO (even down to diameters of only a few hundred kilometers; Barkume et al. 2008) suggests that exotic processes such as cryovolcanism are unlikely to be required. The presence of crystalline water ice on so many small outer solar system bodies may indicate that our current understanding of the physics of the crystalline/amorphous phase transition may not be complete. The spectrum of Quaoar is consistent with that of a cold, geologically dead object slowly losing the last of its volatile ices by escape in a tenuous, perhaps patchy, atmosphere.

Ethane is an expected by-product of irradiation of methane ice (Baratta et al. 2003). The presence of ethane on Quaoar and on 2005 FY9 supports the suggestion of Brown et al. (2007) that these irradiation products are preferentially seen on bodies with large abundances of pure methane rather than on the bodies where the methane is diluted in nitrogen. Quaoar also appears to be rich in more complex irradiation products. Quaoar is the only water ice–rich KBO that has a red color in the visible. Other water ice–rich KBOs like Orcus, Charon, and 2003 EL61 and its family of collisional fragments are all blue in the visible (Barkume et al. 2008). Quaoar's red surface is likely due to the continued irradiation of methane, ethane, and their products on the surface (Brunetto et al. 2006).

While methane on Quaoar is sufficiently volatile that it is likely to seasonally migrate if Quaoar has a moderate obliquity, ethane and the other irradiation products are essentially involatile at Quaoar's temperature. Quaoar is therefore likely to have an irregular covering of irradiation products, perhaps leading to rotational variability in its visible color and in the abundance of ethane. Continued observations of this object will provide insight into the nature of the volatile-nonvolatile transition and atmospheric escape in the outer solar system.

We thank an anonymous referee for a helpful review. E. L. S. is supported by a NASA Graduate Student Research Fellowship. The data presented herein were obtained at the W. M. Keck Observatory, which is operated as a scientific partnership among the California Institute of Technology, The University of California, and the National Aeronautics and Space Administration. The observatory was made possible by the generous financial support of the W. M. Keck Foundation.

REFERENCES

Baratta, G. A., Domingo, M., Ferini, G., Leto, G., Palumbo, M. E., Satorre, M. A., & Strazzulla, G. 2003, Nucl. Instrum. Methods Phys. Res. B, 209, 283
Barkume, K. M., Brown, M. E., & Schaller, E. L. 2008, AJ, in press
Barucci, M. A., Cruikshank, D. P., Dotto, E., Merlin, F., Poulet, F., Dalle Ore, C., Fornasier, S., & de Bergh, C. 2005, A&A, 439, L1
Brown, M. E. 2000, AJ, 119, 977
Brown, M. E., Barkume, K. M., Blake, G. A., Schaller, E. L., Rabinowitz, D. L., Roe, H. G., & Trujillo, C. A. 2007, AJ, 133, 284
Brown, M. E., & Trujillo, C. A. 2004, AJ, 127, 2413
Brown, M. E., Trujillo, C. A., & Rabinowitz, D. L. 2005, ApJ, 635, L97
Brunetto, R., Barucci, M. A., Dotto, E., & Strazzulla, G. 2006, ApJ, 644, 646
Grundy, W. M., & Schmitt, B. 1998, J. Geophys. Res., 103, 25809
Grundy, W. M., Schmitt, B., & Quirico, E. 2002, Icarus, 155, 486
Hapke, B. 1993, Theory of Reflectance and Emittance Spectroscopy (Cambridge: Cambridge Univ. Press)
Jewitt, D. C., & Luu, J. 2004, Nature, 432, 731
Licandro, J., Pinilla-Alonso, N., Pedani, M., Oliva, E., Tozzi, G. P., & Grundy, W. M. 2006, A&A, 445, L35
McBride, N., Green, S. F., Davies, J. K., Tholen, D. J., Sheppard, S. S., Whiteley, R. J., & Hillier, J. K. 2003, Icarus, 161, 501
McLean, I. S., et al. 1998, Proc. SPIE, 3354, 566
Moore, M. H., Ferrante, R. F., Hudson, R. L., & Stone, J. N. 2007, Icarus, 190, 260
Quirico, E., & Schmitt, B. 1997, Icarus, 127, 354
Schaller, E. L., & Brown, M. E. 2007, ApJ, 659, L61
Stansberry, J., Grundy, W., Brown, M., Cruikshank, D., Spencer, J., Trilling, D., & Margot, J.-L. 2007, preprint (astro-ph/0702538)